organics

MDPI

Article

Evaluation of Natural Dye Extracts from African Plants for the Photooxygenation of α-Terpinene to the Anthelmintic Ascaridole

Chinyere Chidimma Enyi [1,2], Gloria Ihuoma Ndukwe [2], Godswill Kuta Fekarurhobo [2,*] and Michael Oelgemöller [1,3,*]

[1] College of Science and Engineering, James Cook University, Townsville, QLD 4811, Australia; chinyere.enyi@ust.edu.ng
[2] Department of Chemistry, Rivers State University, Nkpolu-Oroworukwo, Port Harcourt 500101, Nigeria; gloria.ndukwe@ust.edu.ng
[3] Faculty of Chemistry and Biology, Hochschule Fresenius gGmbH—University of Applied Sciences, 65510 Idstein, Germany
* Correspondence: fekarurhobo.godswill@ust.edu.ng (G.K.F.); michael.oelgemoeller@jcu.edu.au (M.O.)

Abstract

In this study, the singlet oxygen photosensitization potential of three natural African plant extracts was investigated using the photooxygenation of α-terpinene (**1**). Utilizing visible light, the *Carpolobia lutea* extract achieved high conversions towards the anthelmintic ascaridole (**2**) of >60% after 90 min of irradiation, while the extracts of *Hibiscus sabdariffa* and *Justicia secunda* failed to induce significant photoreactivity. Quenching using 1,4-diazabicyclo[2.2.2]octane (DABCO) confirmed a singlet oxygen pathway for irradiation with the *C. lutea* extract. Further separation of the *C. lutea* extract and subsequent photooxygenation screening established several active fractions for ascaridole generation. Advanced HPLC–MS analyses of these active fractions revealed several photosensitizing constituents. These findings establish *C. lutea* extract as a sustainable and effective photosensitiser with comparable performance to commercial dyes.

Keywords: *Carpolobia lutea*; *Hibiscus sabdariffa*; *Justicia secunda*; photooxygenation; singlet oxygen; α-terpinene; ascaridole

1. Introduction

African plants represent a rich resource for natural dyes, pharmaceuticals, and healthcare products [1–3]. Likewise, natural dyes and pigments are known for their biodegradable and non-toxic properties and thus offer a diverse range of applications across industries [4]. Furthermore, many natural dye materials show phototoxic and photosensitizing properties, which makes them interesting for photochemical and -medicinal processes [5]. Of these, photooxygenations involving singlet oxygen ($^1O_2$) represent attractive transformations in organic synthesis [6–10], medicine [11,12], and environmental remediation [13–15]. These reactions generally involve the excitation of a photosensitiser molecule (Sens) by visible or ultraviolet light, enabling the transfer of energy to molecular oxygen to generate singlet oxygen that reacts with a variety of functional groups (Scheme 1) [16,17].

Numerous organic photosensitisers with advantageous physicochemical properties and high quantum yields for $^1O_2$ generation have become commercially available [18,19]. Immobilized solid-supported photosensitizing materials have likewise been developed and allow for rapid removal and recycling [20,21]. Despite these advantages, synthetic dyes possess significant environmental, health, and cost-related threats [22,23]. In contrast,

Academic Editor: Wim Dehaen

Received: 25 November 2025
Revised: 22 December 2025
Accepted: 25 December 2025
Published: 5 January 2026

natural plant-derived dyes are readily available from renewable resources and have found widespread utilization in photodynamic therapy [24,25], dye-sensitized solar cells [26], and photoinitiation [27]. Natural dyes have also been used historically in preparative photooxygenations [28,29].

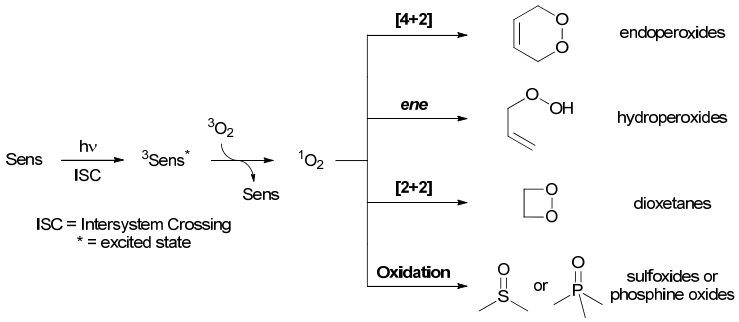

Scheme 1. Photosensitized generation of singlet oxygen and common photooxygenation reactions.

As part of a completed PhD investigation [30], this study investigated the photosensitizing ability of three African plant extracts for the synthesis of the anthelmintic ascaridole from α-terpinene [31]. *Hibiscus sabdariffa* (roselle), *Carpolobia lutea* (cattle stick), and *Justicia secunda* (blood root) were chosen due to their widespread occurrence in West Africa and the deep colours of their extracts. *H. sabdariffa* is a flowering plant of the genus *Hibiscus*, extensively used as food or beverage, and it shows potential for medical applications [32,33]. Similarly, *C. lutea* is a plant species of the Polygalaceae family and it is used as food and in traditional medicine [34,35]. *J. secunda* belongs to the family of Acanthaceae and finds broad applications in traditional folk medicine [36,37].

2. Materials and Methods

2.1. General Information

The α-Terpinene (≥89%) was purchased from Merck Life Science Pty Ltd. (Bayswater, VIC, Australia). Gas chromatographic analysis revealed p-cymene (**3**), o-cymene, m-cymene, α-phellandrene, 1,4-cineole, and ascaridole (**2**) as major impurities [38].

Irradiations were carried out in a Rayonet RPR-200 chamber reactor (Southern New England Ultraviolet Company, Brandford, CT, USA) equipped with 16 × 8 W cool white fluorescent tubes (F8W/TS/33-640; Feilo Sylvania International Group Kft., Budapest, Hungary) and in Pyrex Schlenk flasks. Oxygen gas was supplied through a gas-inlet tube.

Column chromatography was carried out in Pyrex glass columns using Scharlau silica gel 60 (0.06–0.2 mm, 70–230 mesh ASTM; Merck Life Science Pty Ltd., Bayswater, VIC, Australia) and gradient elution with ethyl acetate and cyclohexane.

Nuclear magnetic resonance (NMR) spectroscopy was performed on a Bruker 400 AscendTM (^{1}H: 400 MHz and ^{13}C: 100 MHz). Samples were prepared in $CDCl_3$ (δ = 7.26/77.3 ppm), and the residual solvent peak was used as a reference.

GC–FID analyses were conducted using a 7890A GC system by Agilent Technologies (Santa Clare, CA, USA) equipped with an 7683B auto-injector and an Agilent J&W GC column (DB-5ms Ultra Inert, model 122-5532UI, 30 m length, 0.25 mm ID × 0.25 µm film thickness). UV–Vis spectra were recorded in acetonitrile (HPLC grade) within the wavelength range of 200–800 nm on a Cary 60 UV–Vis Spectrometer (Agilent Technologies).

Advanced LC–MS analyses were performed at the Analytical Research Laboratory of Southern Cross University in Lismore, NSW, Australia. An Agilent Technologies 1260 infinity HPLC system coupled with a 6120 Single Quad mass spectrometer was utilized. A Phenomenex Kinetex C_{18} HPLC column (5 µm, 100 × 4.6 mm) and Milli-Q

water and acetonitrile (HPLC grade), both with 0.005 vol-% trifluoroacetic acid, were used. UV–Vis spectra in the range of 190–600 nm were recorded by a diode array detector (DAD).

Pictures of the photochemical reactor and additional technical and analytical details can be found in the Supplementary Materials.

2.2. Treatment of Plant Materials

2.2.1. Collection, Treatment, and Initial Extraction

All plant materials (Figure 1) were sourced within the Federal Republic of Nigeria in West Africa. Calyces of *H. sabdariffa* were purchased at the Mile 3 market in the local government area of Obio-akpor in Rivers State. The *C. lutea* plant was gathered in Amaranze in the local government area of Isiala Mbano in Imo State. *J. secunda* shrubs were obtained in Orhuwhorun in the Udu local government area of Delta State. *H. sabdariffa* (UPH/P/245) and *J. secunda* (UPH/P/244) were subsequently identified at the herbarium of the University of Port Harcourt, and *C. lutea* (UNN/04/0355D) at the Nsukka herbarium of the University of Nigeria, respectively. Calyces and leaves were carefully collected, cleaned, air dried to a constant weight, and ground using a hand mill.

Figure 1. Collected *H. sabdariffa* calyces (**left**), *C. lutea* plant (**centre**), and *J. secunda* shrub (**right**).

Initially, TLC analyses were conducted with n-hexane, ethyl acetate, and methanol as mobile phases to determine the most suitable solvent for the extraction of dye content. *H. sabdariffa* and *C. lutea* were sequentially extracted following the maceration and *J. secunda* using the microwave-assisted methods [39].

Ground calyces of *H. sabdariffa* (492 g) were defatted twice for 24 h using ethyl acetate (2 × 2000 mL), followed by subsequent double extraction for 48 h each with methanol (2 × 2000 mL). Similarly, ground *C. lutea* leaves (432 g) were defatted with n-hexane (2 × 2000 mL) and extracted with ethyl acetate (2 × 2000 mL). *J. secunda* (30 g) ground leaves were defatted using n-hexane (2 × 250 mL) and extracted twice using 35 vol-% water/methanol (2 × 250 mL) upon microwave heating (750 W; medium–low) for 3 min. The extracts from the defatting processes were discarded, whereas the combined extracts were filtered through a cotton plug and evaporated on a rotary evaporator at 45 °C. The remaining residues were stored in the dark at +3 °C.

2.2.2. Fractional Extraction by Vacuum Liquid Chromatography (VLC)

A dry ethyl acetate extract of *C. lutea* (1.5 g) and 3 g of silica gel 60 (0.06–0.2 mm, 70–230 mesh ASTM) were thoroughly ground together in a mortar. The mixture was carefully transferred to a sintered glass funnel packed to a height of 4.5 cm with 45 g of dry silica gel (grain size 5–40 µm). The content was covered with a layer of dry sand, and the column was connected to a vacuum pump. Gradient elution was sequentially carried out with n-hexane, n-hexane/ethyl acetate mixtures, ethyl acetate, ethyl acetate/methanol, and methanol. Volumes and ratios are provided in the Supporting Materials. The fractions

collected were carefully evaporated to dryness using a rotary evaporator at 45 °C. The residues obtained were stored in the dark at +3 °C.

2.3. Irradiation Procedures

2.3.1. General Photooxygenation Procedure

The α-Terpinene (1.75 mmol) and photosensitizing material (rose bengal disodium: 0.033 mmol; methylene blue: 1 mmol; ANT-COOH: 0.03 mmol; *C. lutea* extract: 10 mg) were combined with acetonitrile (50 mL) in a Schlenk flask (capacity: 60 mL) and the mixture was sonicated for 5 min. The solution was subsequently irradiated while a gentle stream of oxygen gas was passed through it. After 90 min of irradiation, a sample of the reaction mixture (ca. 1.5 mL) was rapidly analysed by GC analysis. Selected photooxygenations were conducted in triplicate to evaluate the reproducibility of the procedure. The reaction mixtures from each of the triplicate studies were combined and the solvent was carefully removed by rotary evaporation (200 mbar, ≤30 °C). Ascaridole was subsequently isolated by column chromatography using a gradient of 0 → 2 → 5 vol-% ethyl acetate in cyclohexane.

Following the general photooxygenation procedure, solutions of α-terpinene (1.75 mmol) and VLC-fraction material (10 mg) in acetonitrile (50 mL) were irradiated independently for 90 min. A sample of the product mixture (ca. 1.5 mL) was subsequently analysed by GC.

2.3.2. Other Irradiation Procedures

To determine possible autooxidation, α-terpinene was further irradiated as described in Section 2.3.1 in the absence of any sensitizing material. A quenching experiment was likewise conducted with *C. lutea* extract (10 mg) and 1,4-diazabicyclo[2.2.2]octane (DABCO; 0.3 mmol) following a slightly modified procedure that uses a mixture of acetonitrile and chloroform (9:1 vol-%) to dissolve DABCO.

The general procedure was further modified to evaluate the photostability of *C. lutea* extract in the absence of **1**. A solution of the extract (5 mg) in acetonitrile (100 mL) was transferred to a larger Schlenk tube (capacity: 150 mL) and irradiated upon O_2 purging for 24 h. Aliquots (ca. 2 mL) of the reaction mixture were taken every 2 h for UV–Vis spectrophotometric analysis.

2.4. Spectroscopic Details

Ascaridole (**2**) and p-cymene (**3**) were identified by NMR spectroscopy, and their spectroscopic details matched previously described data [38,40].

Ascaridole (2) [38]. Yellowish liquid. ^{1}H-NMR (400 MHz, $CDCl_3$): δ (ppm) = 0.87 (d, ^{3}J = 6.8 Hz, 6 H, 2 × CH_3), 1.24 (s, 3 H, CH_3), 1.40 (m, 2 H, CH_2), 1.79 (sept, ^{3}J = 6.8 Hz, 1 H, CH), 1.89 (m, 2 H, CH_2), 6.28 (d, ^{3}J = 8.4 Hz, 1 H, =CH), 6.37 (d, ^{3}J = 8.4 Hz, 1 H, =CH). ^{13}C-NMR (100 MHz, $CDCl_3$): δ (ppm) = 16.8 (q, 1 C, CH_3), 16.9 (q, 1 C, CH_3), 21.1 (q, 1 C, CH_3), 25.4 (t, 1 C, CH_2), 29.2 (t, 1 C, CH_2), 31.8 (d, 1 C, CH), 74.0 (s, 1 C, COO), 79.4 (s, 1 C, COO), 132.7 (d, 1 C, =CH), 136.1 (d, 1 C, =CH).

p-Cymene (3) [40]. In mixture with **2**. ^{1}H-NMR (400 MHz, $CDCl_3$): δ (ppm) = 1.25 (d, ^{3}J = 6.8 Hz, 6 H, 2 × CH_3), 2.34 (s, 3 H, CH_3), 2.89 (sept, ^{3}J = 6.8 Hz, 1 H, CH), 7.14 (m, 4 H, CH_{arom}).

3. Results and Discussion

3.1. Extraction of Plant Materials

After the initial defatting process, extractions of the plant materials gave biomass yields of 29% (140.8 g; reddish purple resin) for *H. sabdariffa*, 2% (8.5 g; dark brown viscous oil) for *C. lutea*, and 23% (7.0 g; deliquescent reddish-brown resin) for *J. secunda*. Alarcón-

Alonso et al. and Banwo and co-workers obtained similar yields of 28.3% and 32.2% from the extraction of *H. sabdariffa* with water and methanol, respectively [41,42]. The percentage amount of the ethyl acetate extract of *C. lutea* was likewise comparable to the reported value of 3.5% by Nwindu et al. [43], but higher than that of 0.3% described by Akpan and co-workers [44]. In contrast, the biomass yield obtained for *J. secunda* was larger than the 10.7% by maceration with 80 vol-% MeOH/H_2O reported by Onoja et al. [45], and 10.2% with 70 vol-% MeOH/H_2O described by Anyasor and co-workers [46]. These variations may be explained by differences in extraction techniques, solvents, or plant materials used.

3.2. Photosensitiser Study

All photooxygenation experiments followed modified batch procedures reported in the literature [38,47]. Irradiations of α-terpinene (**1**) in acetonitrile (Scheme 2) were conducted in a Pyrex vessel in a photochemical chamber reactor equipped with fluorescent tubes. The reaction mixture was constantly purged with a gentle stream of O_2 to deliver the reagent gas and to provide mixing.

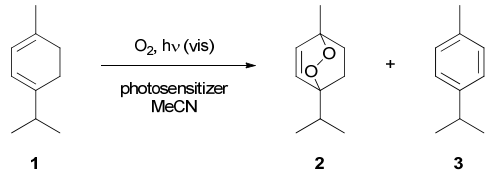

Scheme 2. Photooxygenation of α-terpinene (**1**).

3.2.1. Initial Photosensitiser Study

Initially, screening experiments very conducted with the plant extracts in comparison with common sensitizing materials. Photooxygenations were stopped after 90 min, i.e., before initial GC analysis confirmed complete conversion of **1**. The compositions of each reaction mixture at the beginning (t_0) and after 90 min of irradiation (t_{90}) were subsequently determined by GC (see Supplementary Materials for analytical details). Assignments of the main components were based on the relevant retention times in comparison with pure reference compounds (**1**: 7.08 ± 0.03, **3**: 7.22 ± 0.03, and **2**: 10.97 ± 0.03 min). The differences in amounts (t_{90}–t_0) were calculated, and the results are summarized in Table 1 together with the experimental details.

Table 1. Experimental details and results (**1**: 89%, 0.267 g, 1.75 mmol; cool white; Pyrex; 90 min).

Entry	Sensitizer			Changes in Composition [1]		
	Type	Amount (mg)	Activity	1 (%)	2 (%)	3 (%)
1	Rose bengal	33	++	−69.4	+59.6	+4.0
2	Methylene blue	33	++	−65.8	+59.9	+2.5
3	ANT-COOH	8	+	−37.7	+3.3	+19.7
4	*H. sabdariffa* extract	10	− −	−3.6	+2.8	+0.6
5	*C. lutea* extract	10	++	−65.3	+62.3	+4.3
6	*J. secunda* extract	10	−	−8.8	+5.0	+0.2
7	None		− −	−4.9	+0.8	+2.6
8	*C. lutea* extract [2]	10 (34 [3])	+	−32.3	+12.4	−0.6

[1] Determined by GC analysis (±0.5%). [2] With 10 vol-% chloroform. [3] Amount of DABCO added.

Ascaridole (**2**) is known to be generated through [4+2]-cycloaddition with singlet oxygen [31,38]. Under all irradiation conditions, however, the formation of **2** was accompanied by p-cymene (**3**) in varying amounts. Its formation has been suggested to occur

through thermal autoxidation of **1** [48], breakdown of intermediary hydroperoxides [49], decomposition of ascaridole (**2**) [50], or photoinduced electron-transfer [51].

The use of rose bengal and methylene blue as established sensitizers furnished consumptions of **1** of 69.4 and 65.8% (entries 1 and 2), respectively. In both cases, the amounts of ascaridole (**2**) increased significantly by 59.6 and 59.9%, while those of p-cymene (**3**) rose slightly by 4.0 and 2.5%. As is supported by many studies [31,38,40,47,52], these sensitizers generate ascaridole through the addition of $^1O_2$ to **1**. For example, with rose bengal under comparable conditions, Ronzani et al. reported amounts of ascaridole and p-cymene of 78 and 14%, respectively [38].

Irradiation in the presence of anthraquinone-2-carboxylic acid (ANT-COOH) resulted in a low conversion of α-terpinene (**1**) of approx. 38% (entry 3). The reaction proceeded more sluggishly with increases in ascaridole (**2**) of 3.3% and, more significantly, of p-cymene (**3**) of 19.7%, respectively. Ronzani and co-workers also observed predominant photodehydrogenation of **1** to p-cymene (**3**) and further identified several major side products [38]. In contrast to $^1O_2$ photosensitisers, ANT-COOH is known to initiate photooxidations via an electron transfer mechanism, which subsequently leads to the formation of **3** as the main photoproduct [53,54].

H. sabdariffa extract failed to induce any significant transformations. At the end of the irradiation, a neglectable conversion of **1** of <4% was noted, accompanied by the formation of products **2** and **3** in very low amounts (entry 4).

When using *C. lutea* extract, photooxygenation went smoothly instead and a conversion of **1** of ca. 65% was reached (entry 5). The proportion of ascaridole (**2**) significantly increased by 62.3%, thus resulting in a selectivity of 95%. In contrast, the amount of p-cymene (**3**) rose only slightly by 4.3%. These values are comparable to those obtained with the traditional sensitizers rose bengal and methylene blue (entries 1 and 2), suggesting efficient $^1O_2$ generation by *C. lutea* extract.

In contrast, the use of *J. secunda* extract resulted in a low conversion of α-terpinene (**1**) of just about 9% (entry 6). The amount of ascaridole (**2**) increased by 5%, while that of p-cymene (**3**) remained almost constant.

To evaluate the potential formation of **2** and **3** by autooxidation or self-sensitization, an irradiation experiment was conducted in the absence of any sensitizing material (entry 7). After 90 min, the amount of α-terpinene (**1**) had dropped marginally by just about 5%, with the proportions of ascaridole (**2**) and p-cymene (**3**) increasing by 0.8 and 2.6%, respectively. This low conversion suggests that alternative (photo)oxidation processes play only a very minor role. However, more dramatic autooxidations involving α-terpinene (**1**) have also been described [38,48]. In particular, Ronzani and co-workers achieved a conversion of 49% after 150 min of irradiation under sensitizer-free conditions and found an increase in p-cymene (**3**) of 35% with no formation of ascaridole (**2**) [38].

To further verify the photooxygenation reactivity of natural *C. lutea* extract, a $^1O_2$ quenching experiment was performed using 1,4-diazabicyclo[2.2.2]octane (DABCO, entry 8) [55,56]. Irradiation in the presence of 0.07 mmol of DABCO for 90 min resulted in a drop in conversion to approx. 32%, accompanied by a significantly reduced increase in ascaridole (**2**) formation by 12.4%. In contrast, the amount of p-cymene (**3**) remained almost unchanged with only a slight decrease of 0.6%. Similar reductions in photooxygenation efficiencies have been described for other reactions [56]. The retarded formation or even slight degradation of **3** may suggest competing electron-transfer processes involving DABCO and subsequent degradation [57].

3.2.2. Reproducibility Study and Isolation of Ascaridole

All photooxygenations were repeated in triplicate to confirm reproducibility. The amounts of **2** after each irradiation were initially determined by GC analysis (Table 2). From the most effective experimental series, photoadduct **2** was subsequently obtained by chromatography. While the photooxygenation of α-terpinene is widely used as a test reaction for developing new photochemical technologies incl. sensitizers, ascaridole (**2**) is rarely isolated in pure form. As an example, the pioneering study of Schenck and co-workers reported isolated yields of just 25–31% after careful distillation [52]. Instead, the 'yield' of the endoperoxide **2** is typically determined by analytical techniques.

Table 2. Experimental details and results (**1**: 89%, 0.267 g, 1.75 mmol; cool white; Pyrex; 90 min).

Entry	Sensitizer		Proportion of 2 (%) [1]	Isolated Yield of 2 (%) [2]
	Type	Amount (mg)		
1	Rose bengal	33	74.5 ± 4.9	71 (95 [3])
2	Methylene blue	33	69.5 ± 0.7	43 (62 [3])
3	ANT-COOH	8	5.5 ± 0.7	n.d. [4]
4	*H. sabdariffa* extract	10	4.0 ± 0.2	n.d. [4]
5	*C. lutea* extract	10	61.5 ± 2.1	60 (98 [3])
6	*J. secunda* extract	10	2.0 ± 1.4	n.d. [4]
5	*C. lutea* extract [5]	10 (34 [6])	33 ± 2.8	n.d. [4]

[1] Mean value ± SD by GC analysis (±0.5%) of the crude reaction mixture. [2] By column chromatography. [3] Recovery of **2**. [4] not determined. [5] With 10 vol-% chloroform. [6] Amount of DABCO added.

Acceptable-to-high reproducibility rates were achieved in all cases. The larger fluctuation in the case of rose bengal (entry 1) may have been caused by the simple gas feeding mechanism, which impacted oxygen saturation. The need to remove unreacted **1**, major by-product **3,** and other minor impurities by chromatography lowered the isolated yields of **2** to 43–71% (entries 1, 2, and 5) [58]. Most importantly, the experiments involving *C. lutea* extract furnished a good yield of ascaridole (**2**) of 60% (entry 5), corresponding to an excellent recovery of 98%.

3.3. Photostability Testing of C. lutea Extract

The photodecomposition, -oxidation, or -bleaching of dyes are common and thus limit their usability as photosensitisers [59,60]. The photostability of the *C. lutea* extract was thus evaluated under simulated photooxygenation conditions. A greenish-golden solution of the extract (5 mg) in acetonitrile (100 mL) was irradiated for 24 h. Samples were taken every 2 h and were analysed by UV–Vis. Initially, *C. lutea* extract showed a broad absorption between 625 and 724 nm with a maximum (λ_{max}) at 662 nm. Over the course of the experiment, a significant drop in absorbance to 34% and a slight λ_{max} shift to 665 nm were noted (see Supplementary Materials). Although the solution retained a strong golden colour, partial photooxidation of individual *C. lutea* constituents is assumed. Schenk et al. used spinach leaves as photosensitisers for ascaridole production and reported their complete bleaching in sunlight [52]. During solar photooxygenations, photobleaching has been compensated for by the regular refeeding of sensitizer materials [61,62].

3.4. Further Studies on C. lutea Extract

Due to the remarkable photosensitization efficiency of *C. lutea* extract, further fractionation by vacuum liquid chromatograph (VLC) was conducted to obtain fractions with fewer chemical components [63]. The photoreactivities of these were then tested and the main constituents of the most active fractions were determined by advanced HPLC–MS analyses.

3.4.1. Fractionation of *C. lutea* Extract

Applying increasing solvent polarities, VLC produced a total of 13 main fractions (**F1–F13**) in various amounts. Subfractions were further obtained with 10 vol-% of ethyl acetate in n-hexane (**F2a–F2d**), 50 vol-% of ethyl acetate in n-hexane (**F4a,F4b**), and neat ethyl acetate (**F6a,F6b**). The lowest recovery of 2% was obtained with 15 vol-% methanol in ethyl acetate (**F10**), while the highest of 16% was achieved with 20 vol-% ethyl acetate in n-hexane (**F3**). The colours ranged from different shades of yellow to gold and brown. More experimental details are provided in the Supplementary Materials.

3.4.2. Photosensitizing Study

The various fractions obtained by VLC were subsequently tested using the photooxygenation of α-terpinene (**1**). After 90 min of irradiation, the changes in product compositions (t_{90}–t_0) of **1**, ascaridole (**2**), and p-cymene (**3**) were again determined by GC analyses using their corresponding retention times (Table 3).

Table 3. Experimental details and results (**1**: 89%, 0.267 g, 1.75 mmol; VLC fraction material: 10 mg; cool white; Pyrex; 90 min).

Entry	VLC Fraction [1]	Changes in Composition [2]		
		1 (%)	**2 (%)**	**3 (%)**
1	**F1** (hex)	−3.8	+2.4	+5.3
2	**F2a** (hex, 10 vol-% EA)	−33.3	+20.1	+7.0
3	**F2b** (hex, 10 vol-% EA)	−55.3	+31.5	+9.7
4	**F2c** (hex, 10 vol-% EA)	−50.1	+36.7	+2.9
5	**F2d** (hex, 10 vol-% EA)	−58.2	+45.1	+2.7
6	**F3** (hex, 20 vol-% EA)	−40.2	+31.7	+0.2
7	**F4a** (hex, 50 vol-% EA)	−43.3	+36.8	+0.2
8	**F4b** (hex, 50 vol-% EA)	−50.5	+37.6	+0.4
9	**F5** (hex, 70 vol-% EA)	−47.4	+35.1	+0.3
10	**F6a** (EA)	−50.7	+46.3	+1.5
11	**F6b** (EA)	−54.9	+45.5	+0.7
12	**F7** (EA, 2 vol-% MeOH)	−50.9	+40.4	+0.5
13	**F8** (EA, 5 vol-% MeOH)	−48.6	+41.2	+1.4
14	**F9** (EA, 10 vol-% MeOH)	−45.2	+38.2	+0.1
15	**F10** (EA, 15 vol-% MeOH)	−29.8	+16.8	+0.4
16	**F11** (EA, 20 vol-% MeOH)	−30.6	+16.6	+1.5
17	**F12** (EA, 25 vol-% MeOH)	−16.6	+9.2	−0.8
18	**F13** (MeOH)	−0.6	+0.2	−0.2

[1] Fractions' solvents (hex = n-hexane; EA = ethyl acetate; MeOH = methanol). [2] Determined by GC analysis (±0.5%).

The most nonpolar (**F1**; entry 1) and polar fractions (**F13**; entry 18) showed the lowest photochemical reactivities with low consumptions of **1** of <4%. Moderate photoactivities with decreases in **1** of <34% were instead obtained for the subsequent fractions **F2a** (entry 2) and **F10–F12** (entries 15–17). While fraction **F2b** (entry 3) furnished a higher conversion of starting material **1** of approx. 55%, it also gave the highest increase in p-cymene (**3**) of almost 10%. The subsequent fractions **F2c** and **F2d** (entries 4 and 5) behaved similarly but produced less by-product **3** with <3%. In contrast, the moderately polar fractions **F3–F9** (entries 6–14) achieved good consumptions of **1** of up to 55% with high preferences for the desired endoperoxide **2**.

3.4.3. Analyses of the Most Photoactive Fractions

The most photoactive fractions of **F3–F9** as well as **F2d** were selected to determine their chemical compositions. Advanced HPLC–MS analysis revealed a variety of major con-

stituents (Table 4 and Scheme 3). Characteristic or distinctive UV–Vis and MS spectra were checked against the Dictionary of Natural Products database for compound identification and verification, respectively [64].

Table 4. Results from HPLC–MS analysis.

Entry	VLC Fraction	Constituents [1]		
		Rt (min)	M + H	Compound Class
1	**F2d**	5.3	575, 592	Phenolic, possibly phloroglucinol, derivative
		6.5	289	Flavanone derivative
		7.9, 8.1, 8.3	213, 243, 273	Phenolic, including possible xanthone, derivatives
		9.6, 9.8	238, 257, 403, 289	Xanthone derivatives
		11.4	445, 423	Anthraquinone derivative, possibly emodin
		12.3, 12.6	403, 421, 439	Anthraquinone or dianthrone derivatives
		12.9, 13.2	507, 421,437	Dianthrone derivatives
		14.4, 14.8	421, 439	Dianthrone derivatives
		15.6	390, 421	Anthraquinone or dianthrone derivative
		16.0	390, 407, 424	Anthraquinone and methoxy or prenyl flavone derivatives
2	**F3**	2.4	—	Protocatechuic acid
		4.1	—	Phenolic derivative
		4.8	—	Flavonone derivative
		5.3	179	Phenolic, possibly phloroglucinol, derivative
		6.5	289, 287	Flavonone derivative
		7.5, 7.8, 8.2	275, 243, 273, 303	Xanthone, possibly mangiferin type, and flavonone, possibly chromone, derivatives
		11.2, 11.4	423, 445	Xanthone or chromone and anthraquinone derivatives
		12.9	507	Triterpene derivative
		14.5, 14.8, 15.0	405, 423	Dianthrone and anthraquinone derivatives
		15.6, 16.0	405, 421, 423, 651	Dianthrone and anthraquinone derivatives
3	**F4a/b** [2]	2.4	—	Protocatechuic acid
		4.8	301	Flavonone derivative
		6.5	289	Flavonone derivative
		6.8, 7.2	287, 105, 238, 256	Flavone and terpenoid derivatives
		8.8, 9.5	301, 385, 403	Flavonoid and triterpenoid derivatives
		11.2, 11.4	445, 423	Xanthone and anthraquinone derivatives
		12.6, 12.8	105, 238, 256, 507	Dianthrone and triterpene derivatives
		13.5, 14.2	599, 629	Anthraquinone and possibly dianthrone derivatives
4	**F5**	2.4	—	Protocatechuic acid
		4.8	303	Flavonone derivative
		5.3, 5.5, 5.6, 5.8	289	Phenolic and flavonone derivatives
		6.2, 6.5, 6.8	289, 287	Phenolic, flavonone and flavone (flavonoid) derivatives
		7.2–7.9	407, 377, 419	Phenolic and possibly phenolic acid derivatives
		8.7, 9.5	385, 403	Phenolic and possibly triterpene derivatives
		13.3	—	Phenolic derivative
		17.6, 17.9	593	Chlorophyll derivatives
5	**F6a/b** [2]	1.8	—	Gallic acid derivative
		2.5	—	Protocatechuic acid
		3.8, 4.2	449, 433	Flavonoid C-glycosides orientin and vitexin
		4.8, 5.0	359, 417, 491	Flavonone and flavonoid glycosides
		5.5	475	Flavonone C-glycoside
		6.5, 6.8	287	Flavonone glycoside and flavonoid aglycone (tetrahydroxy flavone)
		9.3	349, 362, 380	Terpenoid or amine derivative
		14.3	—	Phenolic derivative
		16.7, 17.1	609	Chlorophyll derivatives
		17.4–18.4	535, 593	Chlorophyll derivatives

Table 4. *Cont.*

Entry	VLC Fraction	Constituents [1]		
		Rt (min)	M + H	Compound Class
6	**F7**	1.8	—	Gallic acid derivative
		2.5	—	Protocatechuic acid
		3.8, 4.2	449, 433	Flavonoid C-glycosides orientin and vitexin
		4.8, 5.0	359, 417, 491	Flavonone and flavonoid glycoside
		5.5	475	Flavonone C-glycoside
		6.5, 6.8	287	Flavonone glycoside and flavonoid aglycone (tetrahydroxy flavone)
		12.1	447, 629	Phenolic derivative
		14.3	—	Phenolic derivative
		16.7–17.7	593, 609	Chlorophyll derivatives
7	**F8**	1.8	—	Gallic acid derivative
		2.5	—	Protocatechuic acid
		3.8, 4.2	449, 433	Flavonoid C-glycosides orientin and vitexin
		4.8, 5.0	359, 417, 491	Flavonone and flavonoid glycoside
		5.5	475	Flavonone C-glycoside
		6.5, 6.8	287	Flavonone glycoside and flavonoid aglycone (tetrahydroxy flavone)
		7.8	270, 275	Phenolic derivative
		12.1	447, 629	Phenolic derivative
		14.3	—	Phenolic derivative
		16.7–17.7	593, 609	Chlorophyll derivatives
8	**F9**	1.8	—	Gallic acid derivative
		2.5	—	Protocatechuic acid
		3.6, 3.8	449	Flavonoid C-glycosides orientin and isomer
		4.2, 4.3	433	Flavonoid C-glycoside vitexin and isomer
		4.8, 5.0	359, 417, 491	Flavonone and flavonoid glycoside
		6.5, 6.8	287	Flavonone glycoside and flavonoid aglycone (tetrahydroxy flavone)
		7.8	270, 275	Phenolic derivative
		8.7	301, 318	Phenolic derivative, possibly lignan
		12.7	507, 573	Methoxy flavone derivative
		14.3	—	Phenolic derivative
		16.7–17.7	593, 609	Chlorophyll derivatives

[1] Determined by HPLC–MS coupled with UV–Vis (see Supplementary Materials for analytical details). [2] Mixed samples.

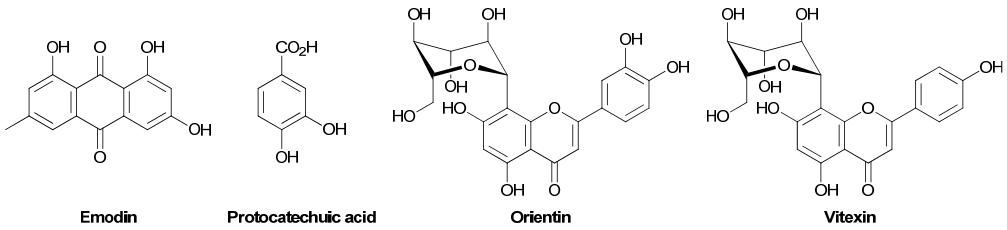

Scheme 3. Examples of proposed constituents of *C. lutea* extracts.

The main constituents detected comprised phenols incl. phloroglucinols, xanthones, anthraquinones and dianthrones, flavonone, flavones and flavonoid derivatives incl. glycosides and aglycones, chromones, and terpenoids. The quinonoid compounds predominantly accumulated in the less polar fractions. In contrast, di- and trihydroxylated benzoic acid and chlorophyll derivatives were identified mainly in the more polar fractions.

So far, only limited isolation attempts and phytochemical profiling have been conducted with *C. lutea* [34]. Alkaloids, saponins, and cardenolides were detected in its plant extracts [65], while the ethyl acetate extract of its roots indicated the occurrence of saponins, anthraquinones, flavonoids, cardiac glycosides, terpenes, and simple sugars [66]. For

the extraction of *C. lutea* leaves with ethyl acetate, Nwidu et al. confirmed the presence of significant phenolic and flavonoid contents [43], whereas Akpan and co-workers reported traces of flavonoids and saponins, moderate amounts of tannins, and high levels of cardiac glycosides, terpenes, and steroids [44]. However, since these analogue studies used chloroform prior to the extraction with ethyl acetate, less-polar compounds such as anthraquinones and dianthrone were likely removed beforehand and hence, could not be detected in significant amounts. Phytochemical screening of ethanolic leaf extracts further revealed saponins, tannins, anthraquinones, cardiac glycosides, and flavonoids as major constituents [67,68]. The essential oil of *C. lutea* leaves has also been analysed and contained terpenoids, hexahydrofarnesyl acetone, (E)-geranyl acetone, (E)-2-decenal, farnesyl acetone, germacrene B, and α-calacorene [35].

Anthraquinones are widely used as photocatalytic materials that can induce electron-transfer or sensitisation processes [69]. Núñez Montoya et al., for example, studied the photosensitization properties of six natural anthraquinones, of which five effectively generated singlet oxygen [70]. Comini and co-workers also demonstrated that the natural anthraquinone parietin has a high $^1O_2$ quantum yield [71]. Likewise, the natural dianthrone hypericin and its derivatives are considered to be highly effective singlet oxygen photosensitisers [72]. Flavonoids are also known for their broad photochemical activity [73,74]. In particular, Suginome and co-workers studied photochemical transformations of flavonoid dehydrorotenoids and postulated the formation of intermediary hydroperoxides via $^1O_2$ self-sensitization [75]. Furthermore, Lv et al. investigated the flavonoid-sensitised photolysis of the fungicide chlorothalonil, and all six flavonoids examined enhanced photodegradation [76]. Porphyrins are well established photosensitisers and have been widely employed in photooxygenation reactions [77,78]. The original ascaridole (**2**) synthesis protocol developed by Scharf, for example, utilized chlorophyl contained in spinach or stinging nettle leaves [9,52]. Additional studies reported on the use of chlorophyll for the photooxygenation of pinenes [79], or the synthesis of the antimalarial agent artemisinin [80]. Phenolic derivatives such as resveratrol and quercetin may also serve as $^1O_2$ generators [81,82]. Lagunes and co-workers, for instance, showed that red wine extracts can act as weak photosensitisers in the photooxidation of ergosterol, which may consequently impact wine-making processing and storage [83]. Shin and co-workers also used octyl gallate as an effective generator of reactive oxygen species in photodynamic therapy [84]. These examples show that the confirmed presence of these photoactive materials contributed to the observed photooxygenation activities of the *C. lutea* extract and its fractions.

4. Conclusions

This study demonstrates that the ethyl acetate extract of *C. lutea* leaves represents an effective natural photosensitiser for the photooxygenation of α-terpinene to the anthelmintic ascaridole with visible light. Fractionation, photochemical screening, and advanced HPLC–MS analyses identified a variety of potent photosensitizing agents. Quenching with DABCO and comparison studies with ANT-COOH confirmed that *C. lutea* extract predominantly functioned as a singlet oxygen generator. *C. lutea* extract may thus serve as a sustainable and renewable photosensitiser for preparative photooxygenations, solar manufacturing, or continuous-flow operations [85–87].

Supplementary Materials: The following supporting information can be downloaded at https://www.mdpi.com/article/10.3390/org7010003/s1. This includes experimental and technical details, analytical data [88], NMR spectra of **2,** and Identification Vouchers. Figure S1. Rayonet chamber reactor during irradiation. Figure S2. Absorbance changes during photostability testing of *C. lutea* extract in acetonitrile. Figure S3. HPLC chromatograms of active *C. lutea* subfractions and UV–Vis spectra of individual components. Table S1. Experimental results of VLC fractionation.

Author Contributions: C.C.E. conducted the research, collected and interpreted the data, and drafted the manuscript; G.I.N. and G.K.F. designed and supervised the research, interpreted the data, and co-drafted and edited the manuscript; M.O. secured the funding, supervised the research, analysed the data, and wrote the final manuscript. All authors have read and agreed to the published version of the manuscript.

Funding: This research was funded by the College of Science and Engineering at James Cook University through a Competitive Research Training Grant 2021.

Data Availability Statement: The original contributions presented in this study are included in the article and its Supplementary Materials. Further inquiries can be directed to the corresponding authors.

Acknowledgments: The authors wish to acknowledge Rivers State University and James Cook University for signing a cotutelle agreement that enabled the success of this research.

Conflicts of Interest: The authors declare no conflicts of interest.

References

1. Wouyou, H.G.; Avocevou-Ayisso, C.; Idohou, R.; Assogbadjo, S.C.; Houndonougbo, J.S.H.; Assogbadjo, A.E. Current Knowledge and Future Prospects of African Plants Providing Natural Dyes: A Systematic Review. *Discov. Plants* **2025**, *2*, 196. [CrossRef]
2. Hostettmann, K.; Marston, A.; Ndjoko, K.; Wolfender, J.-L. The Potential of African Plants as a Source of Drugs. *Curr. Org. Chem.* **2000**, *4*, 973–1010. [CrossRef]
3. Bird, S.R. African Aromatherapy: Past, Present and Future Applications. *Internat. J. Aromather.* **2003**, *13*, 185–195. [CrossRef]
4. Negi, A. Natural Dyes and Pigments: Sustainable Applications and Future Scope. *Sustain. Chem.* **2025**, *6*, 23. [CrossRef]
5. Petit, R.; Izambart, J.; Guillou, M.; da Silva Almeida, J.R.G.; de Oliveira Junior, R.G.; Sol, V.; Ouk, T.-S.; Grougnet, R.; Quintans-Júnior, L.J.; Sitarek, P.; et al. A Review of Phototoxic Plants, Their Phototoxic Metabolites, and Possible Developments as Photosensitizers. *Chem. Biodivers.* **2024**, *21*, e202300494. [CrossRef] [PubMed]
6. Pibiri, I.B.; Piccionello, S.; Palumbo, A.; Pace, A. Photochemically Produced Singlet Oxygen: Applications and Perspectives. *ChemPhotoChem* **2018**, *2*, 535–547. [CrossRef]
7. Ghogare, A.A.; Greer, A. Using Singlet Oxygen to Synthesize Natural Products and Drugs. *Chem. Rev.* **2016**, *116*, 9994–10034. [CrossRef]
8. Clennan, E.L.; Pace, A. Advances in Singlet Oxygen Chemistry. *Tetrahedron* **2005**, *61*, 6665–6691. [CrossRef]
9. Gollnick, K. Photooxygenation and its Application in Industry. *Chim. Ind.* **1982**, *64*, 156–166.
10. Rojahn, W.; Warnecke, H.-U. Die Photosensibilisierte Sauerstoffübertragung—Eine Methode zur Herstellung hochwertiger Riechstoffe. *Dragoco Rep.* **1980**, *27*, 159–164.
11. Anas, A.; Sobhanan, J.; Sulfiya, K.M.; Jasmin, C.; Sreelakshmi, P.K.; Biju, V. Advances in Photodynamic Antimicrobial Chemotherapy. *J. Photochem. Photobiol. C Photochem. Rev.* **2021**, *49*, 100452. [CrossRef]
12. MacDonald, I.; Dougherty, T.J. Basic Principles of Photodynamic Therapy. *J. Porphyr. Phthalocyanines* **2001**, *5*, 105–129. [CrossRef]
13. Al-Nu'airat, J.; Oluwoye, I.; Zeinali, N.; Altarawneh, M.; Dlugogorski, B.Z. Review of Chemical Reactivity of Singlet Oxygen with Organic Fuels and Contaminants. *Chem. Rec.* **2021**, *21*, 315–342. [CrossRef]
14. García-Fresnadillo, D. Singlet Oxygen Photosensitizing Materials for Point-of-Use Water Disinfection with Solar Reactors. *ChemPhotoChem* **2018**, *2*, 512–534. [CrossRef]
15. Marin, M.L.; Santos-Juanes, L.; Arques, A.; Amat, A.M.; Miranda, M.A. Organic Photocatalysts for the Oxidation of Pollutants and Model Compounds. *Chem. Rev.* **2012**, *112*, 1710–1750. [CrossRef] [PubMed]
16. Schmidt, R. Photosensitized Generation of Singlet Oxygen. *Photochem. Photobiol.* **2007**, *82*, 1161–1177. [CrossRef]
17. Foote, C.S. Definition of Type I and Type II Photosensitized Oxidation. *Photochem. Photobiol.* **1991**, *54*, 659. [CrossRef]
18. Fresnadillo, D.G.; Lacombe, S. Reference Photosensitizers for the Production of Singlet Oxygen. In *Singlet Oxygen: Applications in Biosciences and Nanosciences*; Nonell, S., Flors, C., Eds.; The Royal Society of Chemistry: Cambridge, UK, 2016; Chapter 6; Volume 1, pp. 105–143. [CrossRef]
19. Lacombe, S.; Pigot, T. Materials for Selective Photo-oxygenation vs. Photocatalysis: Preparation, Properties and Applications in Environmental and Health Fields. *Catal. Sci. Technol.* **2016**, *6*, 1571–1592. [CrossRef]
20. Lacombe, S.; Pigot, T. New Materials for Sensitized Photo-oxygenation. *Photochemistry* **2011**, *38*, 307–329. [CrossRef]
21. Wahlen, J.; De Vos, D.E.; Jacobs, P.A.; Alsters, P.L. Solid Materials as Sources for Synthetically Useful Singlet Oxygen. *Adv. Synth. Catal.* **2004**, *346*, 152–164. [CrossRef]

22. Rubio, F.T.V.; Maciel, G.M.; Bortolini, D.G.; Fernandes, I.d.A.A.; Pedro, A.C.; Ribeiro, I.S.; Fávaro-Trindade, C.S.; Peralta, R.M.; Haminiuk, C.W.I. Artificial Dyes: Health Risks, Environmental Concerns, and the Rise of Natural Alternatives. *Trends Food Sci. Technol.* **2025**, *162*, 105085. [CrossRef]
23. Alegbe, E.O.; Uthman, T.O. A Review of History, Properties, Classification, Applications and Challenges of Natural and Synthetic Dyes. *Heliyon* **2024**, *10*, e33646. [CrossRef]
24. Gupta, M.; Sahu, A.; Mukherjee, T.; Mohanty, S.; Das, P.; Nayak, N.; Kumari, S.; Singh, R.P.; Pattnaik, A. Divulging the Potency of Naturally Derived Photosensitizers in Green PDT: An Inclusive Review of Mechanisms, Advantages, and Future Prospects. *Photochem. Photobiol. Sci.* **2025**, *24*, 191–214. [CrossRef]
25. Zhou, X.; Ying, X.; Wu, L.; Liu, L.; Wang, Y.; He, Y.; Han, M. Research Progress of Natural Product Photosensitizers in Photodynamic Therapy. *Planta Med.* **2024**, *90*, 368–379. [CrossRef]
26. Dutta, A.; Gohain, B.; Trang, T.T.; Jennings, J.R.; Hao, N.V.; Konwer, S.; Gogoi, A.; Ekanayake, P. Application of Natural Photosensitizers in Dye-sensitized Solar Cells: Opportunities, Challenges, and Future Outlook. *Photochem. Photobiol. Sci.* **2025**, *24*, 1443–1488. [CrossRef]
27. Li, J.; Zhang, Y.; Wu, X.; Lian, H. Research Progress on the Use of Natural Compounds in Photoinitiating Systems. *Huagong Jinzhan Chem. Ind. Eng. Prog.* **2025**, *44*, 941–956. [CrossRef]
28. Oelgemöller, M. Solar Photochemical Synthesis: From the Beginnings of Organic Photochemistry to the Solar Manufacturing of Commodity Chemicals. *Chem. Rev.* **2016**, *116*, 9664–9682. [CrossRef] [PubMed]
29. Coyle, E.E.; Oelgemöller, M. Solar Photochemistry from the Beginnings of Organic Photochemistry to the Solar Production of Chemicals. In *CRC Handbook of Organic Photochemistry and Photobiology*, 3rd ed.; Griesbeck, A., Oelgemöller, M., Ghetti, F., Eds.; CRC Press: Boca Raton, FL, USA, 2012; Chapter 10, Volume 1, pp. 237–247.
30. Enyi, C.C. Plant Extracts as Renewable Resource for Preparative Photooxygenations. Ph.D. Thesis, James Cook University, Townsville, Australia, 2024.
31. Schenck, G.O.; Ziegler, K. Die Synthese des Ascaridols. *Naturwiss* **1944**, *32*, 157. [CrossRef]
32. Cid-Ortega, S.; Guerrero-Beltrán, J.A. Roselle Calyces (*Hibiscus sabdariffa*), an Alternative to the Food and Beverages Industries: A Review. *J. Food Sci. Technol.* **2015**, *52*, 6859–6869. [CrossRef]
33. El Bilali, H. State and Contours of Research on Roselle (*Hibiscus sabdariffa* L.) in Africa. *Open Agric.* **2024**, *9*, 20220336. [CrossRef]
34. Nwidu, L.L.; Nwafor, P.A.; Vilegas, W. The Aphrodisiac Herb Carpolobia: A Biopharmacological and Phytochemical Review. *Phcog. Rev.* **2015**, *9*, 132–139. [CrossRef]
35. Ogunwande, I.A.; Flamini, G.; Avoseh, N.O.; Banwo, I.D. Essential Oil of *Carpolobia lutea*. *Chem. Nat. Compd.* **2014**, *50*, 373–375. [CrossRef]
36. Herrera-Mata, H.; Rosas-Romero, A.; Crescente, C.O. Biological Activity of "Sanguinaria" (*Justicia secunda*) Extracts. *Pharm. Biol.* **2002**, *40*, 206–212. [CrossRef]
37. Świątek, Ł.; Sieniawska, E.; Sinan, K.I.; Zengin, G.; Boguszewska, A.; Hryć, B.; Bene, K.; Polz-Dacewicz, M.; Dall'Acqua, S. Chemical Characterization of Different Extracts of *Justicia secunda* Vahl and Determination of Their Anti-Oxidant, Anti-Enzymatic, Anti-Viral, and Cytotoxic Properties. *Antioxidants* **2023**, *12*, 509. [CrossRef] [PubMed]
38. Ronzani, F.; Costarramone, N.; Blanc, S.; Benabbou, A.K.; LeBechec, M.; Pigot, T.; Oelgemöller, M.; Lacombe, S. Visible-light Photosensitized Oxidation of α-Terpinene using Novel Silica-supported Sensitizers: Photooxygenation vs. Photodehydrogenation. *J. Catal.* **2013**, *303*, 164–174. [CrossRef]
39. Abubakar, A.R.; Haque, M. Preparation of Medicinal Plants: Basic Extraction and Fractionation Procedures for Experimental Purposes. *J. Pharm. Bioallied. Sci.* **2020**, *12*, 1–10. [CrossRef]
40. Ribeiro, S.M.; Serra, A.C.; Rocha Gonsalves, A.M.D. Covalently Immobilized Porphyrins on Silica Modified Structures as Photooxidation Catalysts. *J. Mol. Cat. A Chem.* **2010**, *326*, 121–127. [CrossRef]
41. Alañón, M.E.; Ivanović, M.; Pimentel-Mora, S.; Borrás-Linares, I.; Arráez-Román, D.; Segura-Carretero, A. A Novel Sustainable Approach for the Extraction of Value-added Compounds from *Hibiscus sabdariffa* L. *calyces* by Natural Deep Eutectic Solvents. *Food Res. Internat.* **2020**, *137*, 109646. [CrossRef]
42. Banwo, K.; Sanni, A.; Sarkar, D.; Ale, O.; Shetty, K. Phenolics-Linked Antioxidant and Anti-hyperglycemic Properties of Edible Roselle *(Hibiscus sabdariffa linn.)* Calyces Targeting Type 2 Diabetes Nutraceutical Benefits In Vitro. *Front. Sustain. Food Syst.* **2022**, *6*, 660831. [CrossRef]
43. Nwindu, L.L.; Elmorsy, E.; Thornton, J.; Wijamunige, B.; Wijesekara, A.; Tarbox, R.; Carter, W.G. Anti-Acetylcholinesterase Activity and Antioxidant Properties of Extracts and Fractions of *Carpolobia lutea*. *Pharm. Biol.* **2017**, *55*, 1875–1883. [CrossRef]
44. Akpan, M.M.; Okokon, J.E.; Akpan, E.J. Antidiabetic and Hypolipidemic Activities of Ethanolic Leaf Extract and Fractions of *Carpolobia lutea*. *Mol. Clin. Pharmacol.* **2012**, *3*, 100–107.
45. Onoja, S.O.; Ezeja, M.I.; Omeh, Y.N.; Onwukwe, B.C. Antioxidant, Anti-inflammatory and Antinociceptive Activities of Methanolic Extract of *Justicia secunda* Vahl leaf. *Alex. J. Med.* **2017**, *53*, 207–213. [CrossRef]

46. Anyasor, G.N.; Okanlawon, A.A.; Ogunbiyi, B. Evaluation of Anti-inflammatory Activity of *Justicia secunda* Vahl Leaf Extract using in Vitro and In vivo Inflammation Models. *Clin. Phytosci.* **2019**, *5*, 49. [CrossRef]
47. Shvydkiv, O.; Jähnisch, K.; Steinfeldt, N.; Yavorskyy, A.; Oelgemöller, M. Visible-Light Photooxygenation of α-Terpinene in a Falling Film Microreactor. *Catal. Today* **2018**, *308*, 102–118. [CrossRef]
48. Rudbäck, J.; Bergström, M.A.; Börje, A.; Nilsson, U.; Karlberg, A.-T. α-Terpinene, an Antioxidant in Tea Tree Oil, Autoxidizes Rapidly to Skin Allergens on Air Exposure. *Chem. Res. Toxicol.* **2012**, *25*, 713–721. [CrossRef]
49. Matusch, R.; Schmidt, G. Konkurrenz von Endoperoxid- und Hydroperoxid-Bildung bei der Umsetzung von Singulett-Sauerstoff mit cyclischen, konjugierten Dienen. *Helv. Chim. Acta* **1989**, *72*, 51–58. [CrossRef]
50. Jary, W.G.; Ganglberger, T.; Pöchlauer, P.; Falk, H. Generation of Singlet Oxygen from Ozone Catalysed by Phosphinoferrocenes. *Monatsh. Chem.* **2005**, *136*, 537–541. [CrossRef]
51. Chen, L.; Lucia, L.A.; Gaillard, E.R.; Whitten, D.G.; Icil, H.; Icli, S. Photooxidation of a Conjugated Diene by an Exciplex Mechanism: Amplification via Radical Chain Reactions in the Perylene Diimide-Photosensitized Oxidation of α-Terpinene. *J. Phys. Chem. A* **1998**, *102*, 9095–9098. [CrossRef]
52. Schenck, G.O.; Kinkel, K.G.; Mertens, H.-J. Über die Photosynthese des Askaridols und verwandter Endoperoxyde. *Justus Liebigs Ann. Chem.* **1953**, *584*, 125–155. [CrossRef]
53. Cui, L.; Furuhashi, S.; Tachikawa, Y.; Tada, N.; Miura, T.; Itoh, A. Efficient Generation of Hydrogen Peroxide by Aerobic Photooxidation of 2-Propanol using Anthraquinone-2-carboxylic acid and One-pot Epoxidation of α,β-Unsaturated Ketones. *Tetrahedron Lett.* **2013**, *54*, 162–165. [CrossRef]
54. Jiang, D.; Zhou, W.; Penga, H.; Xie, J.; Liang, S.; Yang, T.; Xie, G.; Wang, B.; Fu, Z.; Su, A. Acidic Photosensitizers Promote the Efficient Photooxygenation of Aromatic Substrates Catalyzed by Anthraquinone-2-carboxylicacid through Proton-coupled Electron Transfer and Particle Aggregation Effect. *Mol. Cat.* **2025**, *578*, 114955. [CrossRef]
55. Li, J.; Wang, L.; Li, J.; Shao, Y.; Liu, Z.; Li, G.; Akkaya, E.U. Taming of Singlet Oxygen: Towards Artificial Oxygen Carriers Based on 1,4-Dialkylnaphthalenes. *Chem. Eur. J.* **2022**, *28*, e202200506. [CrossRef] [PubMed]
56. Ouannes, C.; Wilson, T. Quenching of Singlet Oxygen by Tertiary Aliphatic Amines. Effect of DABCO (1,4-Diazabicyclo[2.2.2]octane). *J. Am. Chem. Soc.* **1968**, *90*, 6527–6528. [CrossRef]
57. Kumar, J.S.D.; Das, S. Photoinduced Electron Transfer Reactions of Amines: Synthetic Applications and Mechanistic Studies. *Res. Chem. Intermed.* **1997**, *23*, 755–800. [CrossRef]
58. Wernerova, M.; Hudlicky, T. On the Practical Limits of Determining Isolated Product Yields and Ratios of Stereoisomers: Reflections, Analysis, and Redemption. *Synlett* **2010**, 2701–2707. [CrossRef]
59. Groeneveld, I.; Kanelli, M.; Ariese, F.; van Bommel, M.R. Parameters that Affect the Photodegradation of Dyes and Pigments in Solution and on Substrate—An Overview. *Dyes Pigment.* **2023**, *210*, 110999. [CrossRef]
60. Demchenko, A.P. Photobleaching of Organic Fluorophores: Quantitative Characterization, Mechanisms, Protection. *Methods Appl. Fluoresc.* **2020**, *8*, 022001. [CrossRef]
61. Esser, P.; Pohlmann, B.; Scharf, H.-D. The Photochemical Synthesis of Fine Chemicals with Sunlight. *Angew. Chem. Int. Ed. Engl.* **1994**, *33*, 2009–2023. [CrossRef]
62. Oelgemöller, M.; Jung, C.; Ortner, J.; Mattay, J.; Zimmermann, E. Green Photochemistry: Solar Photooxygenations with Medium Concentrated Sunlight. *Green Chem.* **2005**, *7*, 35–38. [CrossRef]
63. Anupam, M.; Komal, K.; Subash, C.V.; Ravinder, S.; Anupam, S.K. Vacuum Liquid Chromatography: Simple, Efficient and Versatile Separation Technique for Natural Products. *Org. Med. Chem. Int. J.* **2018**, *7*, 555710. [CrossRef]
64. *Dictionary of Natural Products*; CRC Press: Boca Raton, FL, USA, 2025. Available online: http://dnp.chemnetbase.com (accessed on 25 November 2025).
65. Idowo, P.A.; Jones, O.M.; Herbert, A.O. Phytochemical and Antimicrobial Screening of three Nigerian Medicinal Plants Used to Treat Infectious Diseases Traditionally. *J. Pharm. Biores.* **2005**, *2*, 116–119. [CrossRef]
66. Ettebong, E.O.; Nwafor, P.A.; Ekpo, M.; Ajibesin, K.K. Contraceptive, Estrogenic and Anti-estrogenic Potentials of Methanolic Root Extract of *Carpolobia lutea* in Rodents. *Pak. J. Pharm. Sci.* **2011**, *24*, 445–449.
67. Nwidu, L.L.; Nwafor, P.A. Gastroprotective Effects of Leaf Extracts of *Carpolobia lutea* (polygalaceae) G. Don. in Rats. *Afr. J. Biotechnol.* **2009**, *8*, 12–19.
68. Nwafor, P.A.; Bassey, A.I. Evaluation of Anti-diarrhoeal and Anti-ulcerogenic Potential of Ethanol Extract of *Carpolobia lutea* Leaves in Rodents. *J. Ethnopharm.* **2007**, *111*, 619–624. [CrossRef] [PubMed]
69. Cervantes-González, J.; Vosburg, D.A.; Mora-Rodriguez, S.E.; Vázquez, M.A.; Zepeda, L.G.; Villegas Gomez, C.; Lagunas-Rivera, S. Anthraquinones: Versatile Organic Photocatalysts. *ChemCatChem* **2020**, *12*, 3811–3827. [CrossRef]
70. Núñez Montoya, S.C.; Comini, L.R.; Sarmiento, M.; Becerra, C.; Albesa, I.; Argüello, G.A.; Cabrera, J.L. Natural Anthraquinones Probed as Type I and Type II Photosensitizers: Singlet Oxygen and Superoxide Anion Production. *J. Photochem. Photobiol. B Biol.* **2005**, *78*, 77–83. [CrossRef] [PubMed]

71. Comini, L.R.; Morán Vieyra, F.E.; Mignone, R.A.; Páez, P.L.; Mugas, M.L.; Konigheim, B.S.; Cabrera, J.L.; Núñez Montoya, S.C.; Borsarelli, C.D. Parietin: An Efficient Photo-screening Pigment in Vivo with Good Photosensitizing and Photodynamic Antibacterial effects in Vitro. *Photochem. Photobiol. Sci.* **2017**, *16*, 201–210. [CrossRef]
72. Waser, M.; Falk, H. Progress in the Chemistry of Second Generation Hypericin Based Photosensitizers. *Curr. Org. Chem.* **2011**, *15*, 3894–3907. [CrossRef]
73. Dumur, F. Recent Advances in Visible Light Photoinitiating Systems Based on Flavonoids. *Photochem* **2023**, *3*, 495–529. [CrossRef]
74. Sisa, M.; Bonnet, S.L.; Ferreira, D.; Van der Westhuizen, J.H. Photochemistry of Flavonoids. *Molecules* **2010**, *15*, 5196–5245. [CrossRef]
75. Suginome, H.; Yomezawa, T.; Masamune, T. Photoinduced Oxygenation of Dehydrorotenones. *Tetrahedron Lett.* **1968**, *49*, 5079–5082. [CrossRef]
76. Lv, P.; Min, S.; Wang, Y.; Zheng, X.; Wu, X.; Li, Q.X.; Hua, R. Flavonoid-sensitized Photolysis of Chlorothalonil in Water. *Pest Manag. Sci.* **2020**, *76*, 2972–2977. [CrossRef]
77. Barona-Castaño, J.C.; Carmona-Vargas, C.C.; Brocksom, T.J.; de Oliveira, K.T. Porphyrins as Catalysts in Scalable Organic Reactions. *Molecules* **2016**, *21*, 310. [CrossRef]
78. Dadeko, A.V.; Murav'eva, T.D.; Starodubtsev, A.M.; Gorelov, S.I.; Dobrun, M.V.; Kris'ko, T.K.; Bagrov, I.V.; Belousova, I.M.; Ponomarev, G.V. Photophysical Properties of Porphyrin Photosensitizers. *Opt. Spectrosc.* **2015**, *119*, 633–637. [CrossRef]
79. Kenney, R.L.; Fisher, G.S. Preparation of Trans-Pinocarveol and Myrtenol. *Ind. Eng. Chem. Prod. Res. Develop.* **1973**, *12*, 317–319. [CrossRef]
80. Triemer, S.; Gilmore, K.; Vu, G.T.; Seeberger, P.H.; Seidel-Morgenstern, A. Literally Green Chemical Synthesis of Artemisinin from Plant Extracts. *Angew. Chem. Internat. Ed.* **2018**, *57*, 5525–5528. [CrossRef]
81. Wang, X.; Wang, L.; Fekrazad, R.; Zhang, L.; Jiang, X.; He, G.; Wen, X. Polyphenolic Natural Products as Photosensitizers for Antimicrobial Photodynamic Therapy: Recent Advances and Future Prospects. *Front. Immunol.* **2023**, *14*, 1275859. [CrossRef] [PubMed]
82. Yoshinaga, M.; Toldo, J.M.; Rocha, W.R.; Barbatti, M. Photophysics of Resveratrol Derivatives for Singlet Oxygen Formation. *Phys. Chem. Chem. Phys.* **2025**, *27*, 12560–12568. [CrossRef] [PubMed]
83. Lagunes, I.; Vázquez-Ortega, F.; Trigos, Á. Singlet Oxygen Detection Using Red Wine Extracts as Photosensitizers. *J. Food Sci.* **2017**, *82*, 2051–2055. [CrossRef] [PubMed]
84. Shi, Y.G.; Zhu, C.M.; Li, D.H.; Shi, Z.Y.; Gu, Q.; Chen, Y.W.; Wang, J.-Q.; Ettelaie, R.; Chen, J.S. New Horizons in Microbiological Food Safety: Ultraefficient Photodynamic Inactivation Based on a Gallic Acid Derivative and UV-A Light and Its Application with Electrospun Cyclodextrin Nanofibers. *J. Agric. Food Chem.* **2021**, *69*, 14961–14974. [CrossRef]
85. Wau, J.S.; Robertson, M.J.; Oelgemöller, M. Solar Photooxygenations for the Manufacturing of Fine Chemicals—Technologies and Applications. *Molecules* **2021**, *26*, 1685. [CrossRef]
86. Malakar, P.; Deb, A.R.; Goodine, T.; Robertson, M.J.; Oelgemöller, M. Continuous-flow Photooxygenations: An Advantageous and Sustainable Oxidation Methodology with a Bright Future. In *Catalytic Aerobic Oxidations—Catalysis Series*; Mejía, E., Ed.; Royal Society of Chemistry: Cambridge, UK, 2020; Chapter 7, pp. 181–251. [CrossRef]
87. Cerra, B.; Paccoia, F.; Gioiello, A. Continuous Flow Singlet Oxygen Photooxygenation Reactions: Recent Advances and Applications. *Chimia* **2025**, *79*, 404–410. [CrossRef] [PubMed]
88. Fulmer, G.R.; Miller, A.J.; Sherden, N.H.; Gottlieb, H.E.; Nudelman, A.; Stoltz, B.M.; Bercaw, J.E.; Goldberg, K.I. NMR Chemical Shifts of Trace Impurities: Common Laboratory Solvents, Organics, and Gases in Deuterated Solvents Relevant to the Organometallic Chemist. *Organometallics* **2010**, *29*, 2176–2179. [CrossRef]